

Bromide Adsorption on Ag(001): A Potential Induced Two-Dimensional Ising Order-Disorder Transition

B. M. Ocko,¹ J. X. Wang,² and T. Wandlowski³

¹*Department of Physics, Brookhaven National Laboratory, Upton, New York 11973*

²*Department of Applied Science, Brookhaven National Laboratory, Upton, New York 11973*

³*Department of Electrochemistry, University of Ulm, D-89069 Ulm, Germany*

(Received 25 April 1997)

The adsorption of bromide on an Ag(001) electrode has been investigated using *in situ* x-ray scattering methods. With increasing potential, the bromide undergoes a second order phase transition from a lattice gas to an ordered $c(2 \times 2)$ structure. The order parameter is consistent with the 2D Ising model prediction $\beta = 1/8$. A comparison of x-ray and electrochemical measurements indicates significant lateral disorder at low coverages which decreases with increasing coverage. [S0031-9007(97)03925-2]

PACS numbers: 64.60.Cn, 61.20.Qg

One of the basic tenets in the theory of second order phase transitions is the notion of universality; the critical behavior is determined solely by symmetry and dimensionality. For adsorbates on square substrates, the "Ising" Hamiltonian is $H = V \sum_{ij} n_i n_j - \mu \sum_i n_i$, where V is a lateral interaction parameter, μ is the chemical potential, and the first sum is restricted to nearest neighbors [1]. This model gives rise to an order-disorder (OD) transition and is isomorphic to the Ising spin ($s = 1/2$) model in two dimensions. These two-dimensional (2D) models appear to describe the critical behavior of bulk layered magnetic materials [2]. Here we report the results, for Br electroadsorbed on the Ag(001) surface versus the electrochemical potential, which support the Ising prediction. Previously, studies of adsorbates in the Ising universality class were carried out in vacuum—without direct control of the chemical potential—by dosing the sample to achieve a fixed coverage. The results of these studies, most notably chloride on Ag(001) [3] and oxygen on W(112) [4], support the predictions of the Ising model. An important aspect of the present study is that the competing interactions with the coadsorbed water do not appear to alter the universal aspects of the transition.

For adsorbates on a surface the OD transition corresponds to the formation of a phase with long-range positional order from one with short-range order. If the substrate corrugation potential is weak, the liquid correlation function is described as a conventional 2D liquid. On the other hand, the presence of a strong corrugation potential leads to preferred sites, i.e., a lattice gas. Despite the emerging microscopic understanding of electrode surfaces [5,6], the nature of these disordered states have not been directly confirmed. However, by modeling electrochemical data with simple Hamiltonians, interaction parameters have been estimated assuming lattice gas disordered phases [7,8]. Indeed, in this paper we directly show the existence of a lattice gas phase for Br on Ag(001) at lower coverages ($\theta \leq 0.35$) and an ordered phase at higher coverages.

In a surface x-ray scattering measurement, the structure of the adsorbate can be determined from the diffraction peak positions in reciprocal space and their corresponding intensities [9]. For a single crystal substrate, in the absence of an adsorbate layer, the semi-infinite sum over the atomic layers gives rise to rods of scattering (truncation rods) along the surface normal direction. For Ag(001), these rods (extending along L) are observed at all integer (H, K) when the body-centered-tetragonal unit cell, $a = b = 2.889 \text{ \AA}$ and $c = 4.086 \text{ \AA}$, is used. These features are indicated in Fig. 1(b) and are observed at all potentials. In contrast, diffraction spots at half-order positions only emerge above a critical potential (E_c). Four independent spots at $(1/2, 1/2)$, $(1/2, 3/2)$, $(1/2, 5/2)$, and $(3/2, 3/2)$, along with symmetry equivalents, are observed [see Fig. 1(b)]. This square diffraction pattern, identical to the pattern observed for vapor deposited Cl on Ag(001) using low-energy electron diffraction [3], corresponds to a square bromide packing arrangement, $c(2 \times 2)$, as shown in Fig. 1(a) (right). The neighboring bromides are 4.086 \AA apart and $\theta = 0.5$. No other diffraction features were observed at any potential. In particular, an incommensurate phase such as that observed for Br on Au(001) [10] was never observed. The square packing arrangement of the adsorbed Br adlayer is very different from the hexagonal packing formed on Ag(111) [11,12] and Au(111) [6], and the distorted-hexagonal pattern formed on Au(001) [10]. Electrodeposited chloride and iodide on Ag(001) exhibit the same diffraction features, thus forming the identical $c(2 \times 2)$ phase despite their different respective diameters.

Within the ordered $c(2 \times 2)$ phase, the x-ray diffraction profiles are nearly resolution limited and potential independent. In Fig. 1(c) radial profiles, carried out with a high resolution LiF analyzer, at $E - E_c = 0.03$ and 0.20 V are shown through $(1/2, 1/2, 0.12)$. Although the peak intensities differ by about a factor of 3, the profiles are both well described by Gaussians with a width of 0.0037 \AA^{-1} . These peaks are only slightly broader

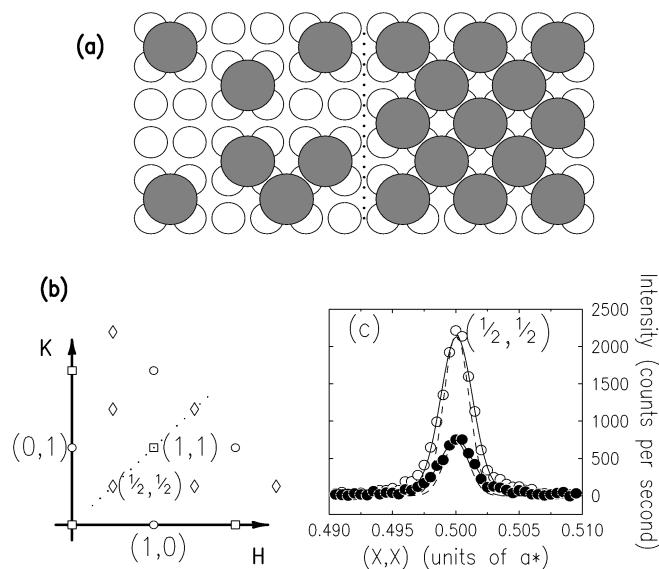


FIG. 1. (a) Real space sketch of the Ag(001) surface (open circles). Bromide is shown adsorbed in a lattice gas configuration (left) and in the commensurate $c(2 \times 2)$ structure (right). (b) In-plane diffraction pattern, where the squares correspond to Bragg peaks, the circles to Bragg rods, and the diamonds to the bromide adlayer. (c) X-ray scattering profiles (circles) in the commensurate phase at 0.03 V (filled circles) and 0.20 V (open circles) positive of the ordering transition. The solid lines are fits to the profiles and the dashed lines are the resolution function.

than the resolution width of 0.0030 \AA^{-1} [13]. The excess width arises primarily from the intrinsic scattering line shape and is about 0.002 \AA^{-1} corresponding to a correlation length of $\approx 2\pi/0.002 \text{ \AA}^{-1} \approx 3000 \text{ \AA}$. Over the entire region $E > E_c$, no profile broadening was observed despite a more than tenfold change in the scattering intensity. Similarly, the transverse correlation lengths are potential independent and also resolution limited. The absence of potential-dependent broadening tends to rule out a model with wandering domain walls between regions with different sublattices. In addition, in the disordered phase, the expected weak critical scattering originating from fluctuations of small ordered patches is obscured by the high background intensity inherent in these measurements.

In Fig. 2 we show the cyclic voltammetry (CV) and the potential-dependent x-ray scattering intensity at $(1/2, 1/2, 0.12)$ and at $(1, 0, 0.12)$ during both sweep directions. Hysteresis, 20–30 mV, is attributed primarily to changes in the surface morphology. The broad weak peak in the CV at about -1.1 V has been attributed to the reorientation of surface water and the second, sharper peak at about (-0.75 V) to a phase transition in the adsorbate layer [14]. On the basis of the potential-dependent scattering at the half-order positions and no other identifiable features below this potential, we identify the rapid increase in the intensity from zero as an OD transition between the two structures shown in Fig. 1(a). At potentials more positive than -0.76 V the scattering intensity (negative sweep) at $(1/2, 1/2, 0.12)$

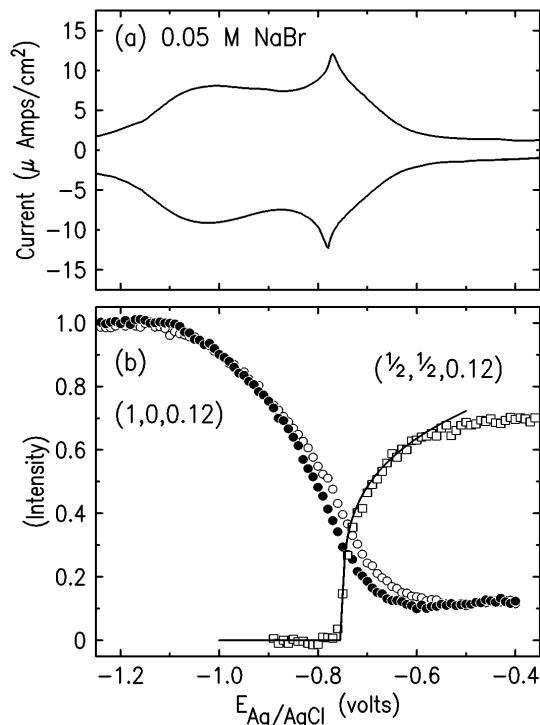


FIG. 2. Comparison of the electrochemical and x-ray scans from the Ag(001) surface in 0.05 M NaBr with the pH adjusted to 10 using NaOH. The cyclic voltammogram (10 mV/sec) shown in (a) was obtained using a separate cell. The diffracted x-ray signals (1 mV/sec) at $(0.5, 0.5, 0.12)$ and $(1, 0, 0.12)$ are shown in (b) after subtracting the diffuse component. Both intensities were normalized by the same factor such that the intensity at $(1, 0, 0.12)$ at -1.2 V was unity. Power-law fits to the $(0.5, 0.5, 0.12)$ signal are shown with exponents $2\beta = 0.25$ (solid line).

starts to rapidly increase from zero as demonstrated by the data shown as squares in Fig. 2(b). This result clearly identifies the sharp peak in the CV with the ordered phase. Saturation occurs at about -0.5 V , corresponding to the potential where the current levels off in the CV.

The x-ray intensity at superlattice positions, such as $(1/2, 1/2)$, measures the order parameter squared [1] and is isomorphic to the staggered magnetization in the Ising spin problem. Thus, the intensity should behave as $(E - E_c)^{2\beta}$ for $E > E_c$ with $\beta = 1/8$. This prediction, shown as the solid line in Fig. 2(b), provides a good description of the critical behavior up to about 80% of the saturation value and clearly supports the Ising prediction for β . The data and fit for the other sweep direction (not shown) are similar, except for an offset of 25 mV, suggesting morphological changes (analogous to shifts in T_c). When β is allowed to vary in the fits, its uncertainty is ± 0.04 . Clearly, the mean-field prediction of $\beta = 1/2$ does not provide a reasonable description of the critical behavior. For Cl on Ag(001) in ultrahigh vacuum, $\beta = 0.12 \pm 0.04$; however, in this study the chemical potential was not directly measured but ascertained from the coverage.

In support of our thesis that the transition is “Ising-like,” similar behavior at the half-order and integer positions

is also found in chloride solutions [15]. The intensity versus potential characteristics exhibit the same power-law behavior. The measured intensity ratio (≈ 4.5) for the two halides at $(1/2, 1/2, 0.12)$ follows the expectations of their respective form factors. This supports our assertion that the potential-dependent diffraction features are not correlated with a rearrangement of the silver atoms.

The power-law form used to describe the order parameter is only asymptotically correct close to the transition, and the saturation observed at high coverages is expected. While exact solutions to the zero-field Ising model exist in 2D, the formalism cannot be applied here because of the presence of an applied field. In addition, the effects of the coverage-dependent indirect interactions [16] would modify the critical behavior far from the transition. Monte Carlo simulations, given the appropriate Hamiltonian, should provide a more exact limiting form.

The nature of the disordered phase is revealed by considering the potential-dependent scattering intensity at $(1, 0, 0.12)$ which is sensitive to both the arrangement of the surface silver atoms and that of the adsorbate layer. As shown in Fig. 2(b), the onset of the slow decrease with increasing potential at about -1.0 V is correlated with the broad peak in the CV. This, however, occurs after the initial increase in the current (e.g., adsorption). Close to the potential where long-range order in the bromide monolayer is established, there is a slight increase in the magnitude of the slope in the intensity at $(1, 0, 0.12)$, but no discontinuity. This, as we shall see, indicates that the coverage changes continuously and supports the notion that the phase transition is close to being second order. At the most positive potentials, where the ordered phase is well developed, the intensity has reached a ratio which is 11% of its value in the absence of bromide. The smooth decrease in the scattering intensity at $(1, 0, 0.12)$ is consistent with a continuous increase in coverage from zero to $1/2$. Since the preferential adsorption on *A*-top sites would give rise to an increase in the intensity, and in twofold sites would have no effect, we conclude that the disordered phase is a lattice gas corresponding to random bromide adsorbed on fourfold hollow sites.

A measure of the coverage of Br atoms in fourfold sites, θ_x , is obtained by examining the scattered x-ray intensity from the Ag(001) surface. In the kinematic approximation, the scattered intensity is given by

$$I(H, K, L) \propto \left| f_{\text{Ag}} \sum_{n=-\infty}^0 e^{in\Psi} + \theta_x f_{\text{Br}} e^{2\pi i(Hx+Ky+Lz)} \right|^2, \quad (1)$$

where the sum is over the semi-infinite silver layers, f_{Ag} and f_{Br} are the atomic form factors of silver and bromide, the phase difference between individual layers $\Psi = \pi(H + K + L)$ [17,18], and the reduced coordinate (x, y, z) is the bromide adsorption site. Considering only the odd rods ($H + K = \text{odd}$), the sum in Eq. (1) reduces to

$$S = \frac{e^{i\pi L/2}}{2 \cos(\pi L/2)}, \quad (2)$$

which gives rise to Bragg peaks for odd L and weak scattering between the Bragg peaks. When limiting the adsorption to fourfold sites this weak rod scattering decreases as θ_x^2 , and the intensity ratio (normalized by its value at $\theta_x = 0$) is given by

$$R(\theta_x, L) = \frac{I(L)_{\theta_x}}{I(L)_{\theta_x=0}} = \left| 1 - \theta_x R \frac{e^{2\pi i L z}}{S} \right|^2, \quad (3)$$

where $R = 73\% \approx Z_{\text{Br}}/Z_{\text{Ag}}$ is the calculated form factor ratio for Br to Ag. Accordingly, we calculate $R(\theta_x = 0.5, L = 0.12) = 10.3\%$, in excellent agreement with the measured ratio of 11% discussed above, thus consistent with the proposed fourfold adsorption model in the $c(2 \times 2)$ phase [19].

Measurements at different L confirm the present structural model in the ordered phase and provide an estimate of the separations between the Ag-Br planes ($cz = 2.30$ Å). This, spacing is close to the 2.4 ± 0.3 Å Br-Au layer spacing measured at the Au(111) surface [20].

In Fig. 3(b) we show the coverage obtained from the negative potential sweep scattering data at $(1, 0, 0.12)$ and Eq. (3), as open circles. As expected, the coverages range from zero at the most negative potentials to $1/2$ at the highest potentials. Despite the OD transition at -0.76 V, there is no associated discontinuous change at this potential. θ_e , measured using chronocoulometry [filled circles in Fig. 3(b)] [21], also ranges from zero to $1/2$. Although there is good agreement at the most positive potentials, θ_x is clearly much less than θ_e at intermediate potentials. As shown in the figure, at the OD transition we find $\theta_x = 0.25$ and $\theta_e = 0.35$. The latter is close to the critical coverage of 0.368 obtained from simulations [22,23] and comparable with the critical coverage of 0.394 obtained for Cl on the Ag(001) surface in vacuum [3]. Thus, the critical coverages do not appear to be greatly affected by the presence of water.

The discrepancy between the x-ray and electrochemical coverages forces us to question the assumption that the bromide atoms reside in fourfold hollow sites. We therefore relax this assumption by incorporating a lateral rms displacement, σ . Such displacements may result from either unbalanced adsorbate-adsorbate or adsorbate-water interactions, most significant in the intermediate coverage regime, or from a weak substrate-adsorbate potential well relative to $k_B T$. The unbalanced adsorbate-water interactions are a manifestation of the requirement to provide optimal water density in the irregularly sized interstitial regions between the bromides. In their simplest form, these interactions give rise to an effective Debye-Waller term whose magnitude is simply related to the measured coverage ratio, $\theta_x/\theta_e = e^{-(|q|\sigma)^2/2}$, where q is the reciprocal space position. As shown in Fig. 3(a), σ obtained in this manner decreases from about 0.9 Å to nearly zero with increasing potential/coverage. To our knowledge,

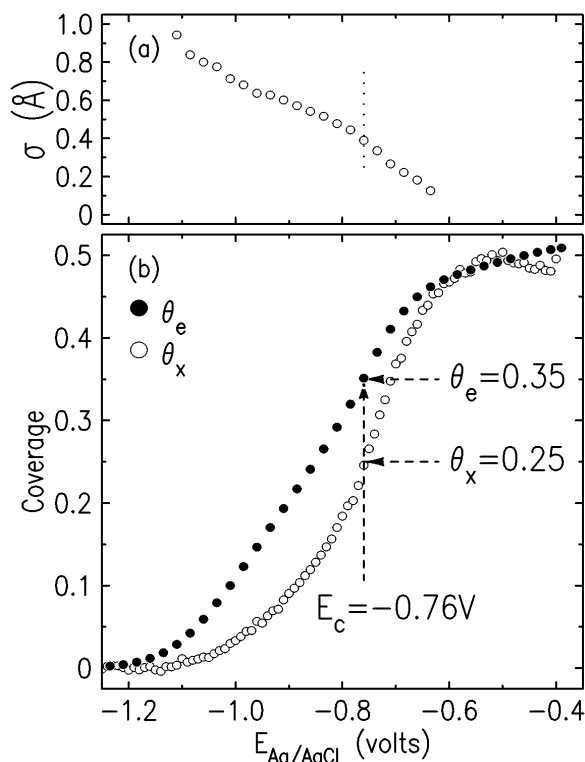


FIG. 3. (b) The coverage: θ_x determined from the analysis of the (1,0,0.12) signal (open circles) and θ_e determined from electrochemical measurements (filled circles). (a) The deviation between these two coverages is analyzed in terms of a lateral displacement amplitude σ , which decreases with increasing coverage.

the corresponding lateral disorder has not been ascertained for adsorbates in vacuum.

Finally, for the Ising Hamiltonian the lateral interaction energy can be estimated from the isotherm using the mean-field approximation. Following the work of van der Eerden [24] with “blocked” near neighbors, the isotherm [Fig. 3(b)] is well described using a repulsive interaction energy of 110 meV between next-nearest neighbor (NNN) adsorbed bromide atoms [21,25]. If this 110 meV effective interaction energy is attributed solely to NNN bromide dipole-dipole interactions, then the dipole moment equals 2.34 D. This is much closer to the gas phase water dipole moment (1.82 D) than the halide values (0.6–0.75 D) found on noble metal surfaces in vacuum [3,26]. The discrepancy with the vacuum value may result from the higher partial charge in the electrochemical environment, the limitations of the mean-field approximation, and from the simplicity of the present model which does not incorporate water-bromide, and water-water interactions.

In conclusion, our x-ray results show that Br forms a lattice gas on the Ag(001) electrode which transforms to an ordered $c(2 \times 2)$ state with increasing potential. The critical coverage and the order parameter exponents are in close agreement with the 2D Ising transition predictions, despite the presence of significant lateral

disorder. We speculate that this disorder results from the unbalanced adsorbate-adsorbate and coadsorbed water-adsorbate interactions. It is hoped that this picture of the order-disorder transition will stimulate a better understanding of fundamental interactions at electrode surfaces.

The work at BNL is made possible by the DOE, under Contract No. DE-AC02-76CH00016. T.W. is supported by the Deutsche Forschungsgemeinschaft (Wa/879/3) and NATO (CRG 961219). We have greatly benefited from our conversations with Ratko Adžić, Steve Feldberg, John Hill, Marc Koper, Eckherd Spohr, and Ian Robinson.

- [1] B. N. J. Person, *Surf. Sci. Rep.* **15**, 1 (1992).
- [2] M. F. Collins, *Magnetic Critical Scattering* (Oxford University Press, Oxford, 1989).
- [3] D. E. Taylor *et al.*, *Phys. Rev. B* **32**, 4653 (1985); R. Q. Hwang *et al.*, *Phys. Rev. B* **37**, 5870 (1988).
- [4] G. C. Wang and T. M. Lu, *Phys. Rev. B* **31**, 5918 (1985).
- [5] M. F. Toney, J. N. Howard, J. Richer, G. L. Borges, and O. R. Melroy, *Phys. Rev. Lett.* **75**, 4472 (1995).
- [6] O. M. Magnussen, B. M. Ocko, J. X. Wang, and R. R. Adžić, *Phys. Rev. B* **51**, 5510 (1995).
- [7] L. Blum and D. A. Hukaby, *J. Chem. Phys.* **94**, 6887 (1991).
- [8] J. Zhang, Y.-E. Sung, P. A. Rikvold, and A. Wieckowski, *J. Chem.* **104**, 5699 (1996).
- [9] I. K. Robinson and D. J. Tweet, *Rep. Prog. Phys.* **55**, 599 (1992).
- [10] B. M. Ocko, O. M. Magnussen, J. X. Wang, and Th. Wandlowski, *Phys. Rev. B* **53**, 7654 (1996).
- [11] B. M. Ocko, O. M. Magnussen, J. X. Wang, R. R. Adžić, and Th. Wandlowski, *Physica (Amsterdam)* **221B**, 238 (1996).
- [12] M. L. Foresti *et al.*, *Surf. Sci.* **335**, 241 (1995).
- [13] The diffraction width of $0.0016a^*$ at (1,0) is slightly broader than the direct beamwidth of $0.0012a^*$.
- [14] G. Valette, A. Hamelin, and R. Parsons, *Z. Phys. Chem.* **113**, 71 (1978).
- [15] B. M. Ocko, J. X. Wang, and T. Wandlowski (to be published).
- [16] T. L. Einstein and J. R. Schrieffer, *Phys. Rev. B* **7**, 3629 (1973).
- [17] H. L. Meyerheim *et al.*, *Surf. Sci.* **304**, 267 (1994).
- [18] T. Tse, P. W. Stephens, and P. J. Eng, *J. Phys. Condens. Matter* **6**, 6111 (1994).
- [19] A Br-Ag layer spacing equal to the Ag-Ag layer spacing was assumed.
- [20] J. Wang, B. M. Ocko, A. J. Davenport, and H. S. Isaacs, *Phys. Rev. B* **46**, 10321 (1992).
- [21] Th. Wandlowski, J. X. Wang, and B. M. Ocko (to be published).
- [22] D. W. Wood and M. Goldfinch, *J. Phys. A* **13**, 2781 (1980).
- [23] W. Kinzel and M. Schick, *Phys. Rev. B* **24**, 324 (1981).
- [24] J. P. van der Eerden *et al.*, *Surf. Sci.* **82**, 364 (1979).
- [25] The measured electrodesorption valence [21], $\gamma = -0.7$, was used.
- [26] P. J. Goddard, K. Schwaha, and R. M. Lambert, *Surf. Sci.* **71**, 351 (1978).